Eur. Phys. J. C 53, 281–287 (2008)
DOI 10.1140/epjc/s10052-007-0447-8

THE EUROPEAN PHYSICAL JOURNAL C

Regular Article – Theoretical Physics

Production of the charged top-pions from TC2 model at the TeV energy $e^-\gamma$ colliders

Yao-Bei Liu[1,a], Xue-Lei Wang[2]

[1] Henan Institute of Science and Technology, Xinxiang 453003, P.R. China
[2] College of Physics and Information Engineering, Henan Normal University, Xinxiang 453007, P.R. China

Received: 30 June 2007 / Revised version: 4 September 2007 /
Published online: 10 November 2007 –

Abstract. The top-pions $(\Pi_t^{0,\pm})$ and the top-Higgs (h_t^0) are the typical particles predicted by the topcolor-assisted technicolor (TC2) model and the observation of these particles can be regarded as direct evidence of the TC2 model. In this paper, we study three pair production processes of these new particles at the next generation $e\gamma$ colliders, i.e., $e^-\gamma \to e^-\Pi_t^+\Pi_t^-$, $e^-\gamma \to \nu_e\Pi_t^-\Pi_t^0$ and $e^-\gamma \to \nu_e\Pi_t^- h_t^0$. The results show that the production rates can reach the level 10^0–10^1 fb with reasonable parameter values. So one can expect that enough signals could be produced in future high- energy linear collider experiments. Furthermore, the flavor-changing (FC) decay modes $\Pi_t^- \to b\bar{c}$, $\Pi_t^0(h_t^0) \to t\bar{c}$ can provide us with the typical signal to detect these new particles.

PACS. 12.60Nz; 14.80.Mz; 12.15.LK; 14.65.Ha

1 Introduction

The standard model (SM) provides an excellent effective field theory description of almost all particle physics experiments. But the Higgs boson mass suffers from an instability under radiative corrections in the SM. A natural argument suggests that the cutoff scale of the SM is not much above the electroweak scale: new physics will appear around TeV energies. Most extensions of the SM require the introduction of an extended Higgs sector to the theory. Generically, a charged Higgs boson arises in the extended Higgs sector, which does not exist in the SM. It implies that the observation of a charged Higgs boson is clear evidence for the existence of new physics beyond the SM.

Dynamical electroweak symmetry breaking (EWSB), such as technicolor (TC) theory [1, 2], is an attractive idea that avoids the shortcomings of the triviality and unnaturalness arising from the elementary Higgs field in the SM. The simplest QCD-like TC models [3–5] lead to a large oblique correction to the electroweak parameter S [6] and is already ruled out by the CERN e^+e^- collider LEP precision electroweak measurement data [7, 8]. Various improvements have been made to make the predictions consistent with the LEP precision measurement data. Among all these improved TC models, the topcolor-assisted technicolor (TC2) model [9–12] is a more realistic one, which provides us with an additional source of EWSB and also solves the heavy top quark problem. In TC2 theory, the new strong dynamics topcolor is assumed to be chiral critically strong at the scale 1 TeV, and it is coupled preferentially to the third generation. In this model, the EWSB is driven mainly by TC interactions and extended technicolor gives the contributions to all ordinary quark and lepton masses including a very small portion of the top quark masses: $m_t' = \varepsilon m_t (0.03 \le \varepsilon \le 0.1)$ [13]. The topcolor interactions also make small contributions to the EWSB and give rise to the main part of the top mass, $(1-\varepsilon)m_t$. Three pseudo-Goldstone bosons (PGBs) called top-pions $\Pi_t^0, \Pi_t^\pm$ and an isospin-singlet boson called the top-Higgs (h_t^0) are predicted by the TC2 model in the few hundred GeV region. These bosons can be regarded as the typical feature of TC2 model. Thus, studying the possible signatures of these typical particles in the present and future high-energy experiments would provide us with crucial information for EWSB and fermion flavor physics. Furthermore, the discovery of these new particles can be regarded as direct evidence to test the TC2 model. A comprehensive review on the phenomenological studies in TC2 model has been given in [14].

The new particles predicted by the TC2 model can be probed directly via its decay modes. The decay modes of the neutral top-pion are the tree-level decay process $\Pi_t^0 \to t\bar{t}$ (if this is kinetically allowed), $\Pi_t^0 \to t\bar{c}$, $\Pi_t^0 \to b\bar{b}$ and the process $\Pi_t^0 \to \gamma\gamma$, gg, γZ through an internal top quark loop. The branching ratios of these possible decay modes have been calculated in detail [15]. The results show that the neutral top-pion almost decays to $t\bar{t}$

[a] e-mail: hnxxlyb2000@sina.com

if the mass of the neutral top-pion M_{Π} is larger than $2m_t$. If $m_t + m_c < M_{\Pi} < 2m_t$, the flavor-changing mode $\Pi_t^0 \to t\bar{c}$ will become the dominant decay mode and the branching ratio may be over 60%. Such a flavor-changing mode can play an important role in the search of the neutral top-pion due to the clean background. For the top-Higgs, a different case is that there exist tree-level decay modes ZZ, W^+W^-. For the charged top-pions, its decay modes have been studied in [16]. The main modes are the tree-level $\Pi_t^+ \to t\bar{b}$ and $\Pi_t^+ \to c\bar{b}$. The alternative way to probe the top-pions and top-Higgs is to study the production mechanism of these particles. The future linear colliders will provide an almost unique place to explore the top-pion due to its clean environment and high luminosity [17–24].

The future e^+e^- colliders can also operate in the $e\gamma$ or $\gamma\gamma$ modes. High energy photons for $\gamma\gamma, e\gamma$ collisions can be obtained using Compton backscattering of laser light off the high-energy electrons. In this case, the energy and luminosity of the photon beam would be of the same order of magnitude as the parent electron beam and the set of final states at a photon collider is much richer than that in the e^+e^- mode. At the same time, the high energy photons polarizations can relatively easily vary, which is advantageous for experiments. All the virtues of the photon colliders will provide us with a good chance to pursuit new physics particles. The production of the neutral top-pion in TC2 at $e\gamma$ colliders has been studied in [25, 26]. Because the SM predicts the existence of one neutral Higgs boson, distinguishing of a Higgs-like neutral top-pion with the Higgs in the SM needs a more precise measurement, but any observation of charged Higgs or Higgs-like particles will mean the signal of new physics. Therefore, probing of charged top-pions is more important to test the TC2 model. At e^+e^- colliders, the main single charged top-pion production processes are $e^+e^- \to t\bar{b}\Pi_t^-$ and $e^+e^- \to W^+\Pi_t^-$, and these process have been systematically studied [15, 27, 28]. In general, the cross sections of the above processes are at the level of 10^0–10^1 fb, and it is promising to observe the top-pions at future linear colliders with high luminosity. Also, the charged top-pion production processes at the photon collider have been studied in [29–31]. In this paper, we will show that the charged top-pions can also be copiously produced via the processes $e^-\gamma \to e^-\Pi_t^+\Pi_t^-$ and $e^-\gamma \to \nu_e\Pi_t^-\Pi_t^0\left(h_t^0\right)$. With reasonable values of the parameters, the production cross sections may reach the level of 10^0–10^1 fb. On the other hand, the production cross sections of charged top-pions via $e^{\pm}\gamma$ scattering are about one order of magnitude larger than those of some similar processes in the minimal supersymmetric standard model (MSSM) [32]. So, we can easily distinguish the charged top-pions from other charged Higgs bosons in MSSM.

This paper is organized as follows. The relevant couplings of the charged top-pions $\Pi_t^{\pm}$ are summarized in Sect. 2. Sections 3 and 4 are devoted to the computation of the production cross sections of the processes $e^-\gamma \to e^-\Pi_t^+\Pi_t^-$ and $e^-\gamma \to \nu_e\Pi_t^-\Pi_t^0\left(h_t^0\right)$. Some phenomenological analyses are also included in the two sections. The conclusions are given in Sect. 5.

2 The relevant couplings of the charged top-pions $\Pi_t^{\pm}$

The TC2 model, incorporating the best features of technicolor and topcolor, offers a new insight into the possible mechanism of EWSB and the origin of the heavy top quark mass. At the EWSB scale, this model predicts two groups of scalars, corresponding to the technicolor condensates and topcolor condensates, respectively. Either of them can be arranged into a SU(2) doublet [33], and their roles in the TC2 model are quite analogous to the Higgs fields in the model proposed in [34], which is a special two-Higgs-doublet model in essence. Explicitly speaking, the doublet Φ_{TC}, which corresponds to the topcolor condensates plays a minor role in EWSB and only couples to the third generation quarks, its main task is to generate the large top quark mass. While the doublet Φ_{ETC}, which corresponds to the technicolor condensates, is mainly responsible for EWSB and the light fermion masses, it also contributes a small portion of top quark mass. The vacuum expectation value (VEV) of the top quark pair condensate f_π can be given by the Pagel–Stokar formula. For condensation around the EWSB scale of 1 TeV, f_π should be near 60 GeV. Once f_π is fixed, the VEV of the technifermion condensates, v_T, is uniquely determined by the EWSB requirement $f_\pi^2 + v_T^2 = v^2 \simeq (246\,\mathrm{GeV})^2$. For $f_\pi = 60$ GeV, we must have $v_T = 239$ GeV. We linearize the theory and rearrange the pions in two orthogonal linear combinations to form the longitudinal degrees of freedom of the weak gauge bosons and a triplet of top-pions, $\Pi^{0,\pm}$, which become physical degrees of freedom.

The mass splitting between the neutral top-pion and the charged top-pions should be small, since such a splitting comes only from the electroweak interactions [35]. References [9–12] have estimated the masses of the top-pions using the quark loop approximation and showed that the masses are allowed to be a few hundred GeV in the reasonable parameter space. Besides physical top-pions, there are two other CP-even Higgs modes, labeled h_t^0 and H_{ETC}, known as the top-Higgs boson and the techni-Higgs bosons, respectively. Their masses can be estimated in the Nambu–Jona-Lasinio (NJL) model in the large N_c approximation [36–38] and is found to be about $2m_t$ [39, 40]. This estimate is also rather crude and the mass below the $t\bar{t}$ threshold is quite possible in a variety of scenarios. On the experimental side, the current experiments have restricted the masses of the charged top-pions. For example, the absence of $t \to \Pi_t^+ b$ implies that $m_{\Pi_t^+} > 165$ GeV [41] and analysis of R_{b} yields $m_{\Pi_t^+} > 220$ GeV [42]. For the masses of the neutral top-pion and top-Higgs, the experimental restrictions on them are rather weak. The direct search for the neutral top-pion (top-Higgs) via $pp \to t\bar{t}\Pi_t^0\left(h_t^0\right)$ with $\Pi_t^0\left(h_t^0\right) \to b\bar{b}$ has been proved to be hopeless at Tevatron with a top-pion (top-Higgs) heavier than 120 GeV [33]. In our following discussions, we will neglect the mass difference among the top-pions and denote their mass as M_{Π}. From the kinetic terms of the effective TC2 Lagrangian in linearized

form [33]

$$L_{\rm kin} = (D_\mu \Phi_{\rm TC})^\dagger (D^\mu \Phi_{\rm TC}) + (D_\mu \Phi_{\rm ETC})^\dagger (D^\mu \Phi_{\rm ETC}) \,, \tag{1}$$

we know that there exist tree-level couplings of the charged top-pions Π_t^- to other particles, which are related to our calculation can be written as [33]

$$Z_\mu \Pi_t^- \Pi_t^+ : \quad \frac{e}{s_{\rm W} c_{\rm W}} \left(1 - 2s_{\rm W}^2\right) \left(p_\mu^- - p_\mu^+\right) \,, \tag{2}$$

$$A_\mu \Pi_t^- \Pi_t^+ : \quad e \left(p_\mu^- - p_\mu^+\right) \,, \tag{3}$$

$$W^{+\mu} \Pi_t^- \Pi_t^0 : \quad -\frac{e}{2s_{\rm W}} \left(p_\mu^- - p_\mu^0\right) \,, \tag{4}$$

$$W^{+\mu} \Pi_t^- h_t^0 : \quad \frac{{\rm i}e}{2s_{\rm W}} \frac{v_T}{v} \left(p_\mu^- - p_\mu^0\right) \,. \tag{5}$$

Here $s_{\rm W} = \sin\theta_{\rm W}$, $c_{\rm W} = \cos\theta_{\rm W}$, and $\theta_{\rm W}$ is the Weinberg angle.

In the TC2 model, the top-color gauge bosons include the topcolor gauge boson B_μ^A and the extra U(1) gauge boson Z'. These gauge bosons have very large masses, which can be up to several TeV. Such large masses will depress the contribution to the cross sections. So, in our calculation, we can neglect the contributions of these gauge bosons. There should be another production $e^-\gamma \to e^- H_{\rm ETC} \Pi_t^-$, but the cross section of such a process is strongly depressed by the factor $\frac{f_\pi}{v}$ and the heavy $H_{\rm ETC}$. On the other hand, techni-Higgs is not the typical particle of the TC2 model. So, we do not study this process in this paper.

3 The process $e^-\gamma \to e^- \Pi_t^+ \Pi_t^-$

The charged top-pions pair $\Pi_t^+ \Pi_t^-$ can be produced via $e^-\gamma$ collision associated with an electron as shown in Fig. 1. Such a process is very important in searching for the charged top-pions because it can produce the distinct signals of the charged top-pions. The invariant production amplitudes of the process $e^-(p_1)\gamma(p_2) \to e^-(p_3)\Pi_t^+(p_4)\Pi_t^-(p_5)$ can be written as

$$M = M_a + M_b + M_c + M_d \,, \tag{6}$$

with

$$\begin{aligned} M_a = {} & {\rm i}e^3 G(p_5 - p_2, M_\Pi) \bar{u}(p_3) \gamma_\mu \\ & \times \left\{ -G(p_1 - p_3, 0) + \frac{(1 - 2s_{\rm W}^2)}{4 s_{\rm W}^2 c_{\rm W}^2} \right. \\ & \left. \times\, G(p_1 - p_3, M_Z)[(-1 + 4s_{\rm W}^2) + \gamma_5] \right\} \\ & \times u(p_1) g^{\mu\nu} (p_5 - p_2 - p_4)_\nu (2p_5 - p_2)^\rho \epsilon_\rho(p_2) \,, \end{aligned} \tag{7}$$

$$\begin{aligned} M_b = {} & {\rm i}e^3 G(p_3 - p_2, 0) \bar{u}(p_3) \not{\epsilon}(p_2) (\not{p}_3 - \not{p}_2)(\not{p}_5 - \not{p}_4) \\ & \times \left\{ G(p_4 + p_5, 0) + \frac{(1 - 2s_{\rm W}^2)}{4 s_{\rm W}^2 c_{\rm W}^2} \right. \\ & \left. \times\, G(p_4 + p_5, M_Z)[(-1 + 4s_{\rm W}^2) + \gamma_5] \right\} u(p_1) \,, \end{aligned} \tag{8}$$

$$\begin{aligned} M_c = {} & {\rm i}e^3 G(p_1 + p_2, 0) \bar{u}(p_3) \gamma_\mu \\ & \times \left\{ -G(p_4 + p_5, 0) + \frac{(1 - 2s_{\rm W}^2)}{4 s_{\rm W}^2 c_{\rm W}^2} \right. \\ & \left. \times\, G(p_4 + p_5, M_Z)[(-1 + 4s_{\rm W}^2) + \gamma_5] \right\} \\ & \times (\not{p}_1 + \not{p}_2) \not{\epsilon}(p_2) u(p_1) g^{\mu\nu} (p_5 - p_4)_\nu \,, \end{aligned} \tag{9}$$

$$\begin{aligned} M_d = {} & {\rm i}e^3 G(p_4 - p_2, M_\Pi) \bar{u}(p_3) \gamma_\mu \\ & \times \left\{ -G(p_1 - p_3, 0) + \frac{(1 - 2s_{\rm W}^2)}{4 s_{\rm W}^2 c_{\rm W}^2} \right. \\ & \left. \times\, G(p_1 - p_3, M_Z)[(-1 + 4s_{\rm W}^2) + \gamma_5] \right\} \\ & \times u(p_1) g^{\mu\nu} (p_5 - p_2 + p_4)_\nu (p_2 - 2p_4)^\rho \epsilon_\rho(p_2) \,, \end{aligned} \tag{10}$$

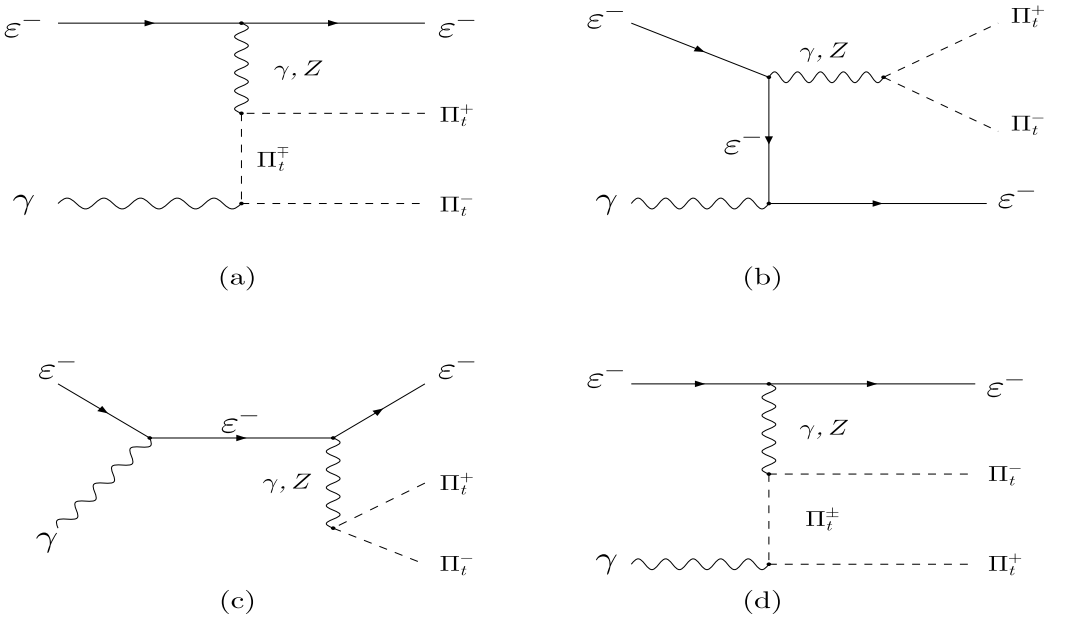

Fig. 1. The Feynman diagrams of the process $e^-\gamma \to e^-\Pi_t^+\Pi_t^-$

where $G(p,M)=\frac{1}{p^2-M^2}$ denotes the propagator of the particles and $\epsilon_\rho(p_2)$ is the polarization vector of the photon, p_4 and p_5 denote the momenta of the outgoing charged top-pions Π_t^+ and Π_t^-.

The hard photon beam of the $e\gamma$ collider can be obtained from laser backscattering at the e^+e^- linear collider. Let $\hat{s}$ and s be the center-of-mass energies of the $e\gamma$ and e^+e^- systems, respectively. After calculating the cross section $\sigma(\hat{s})$ for the subprocess $e^-\gamma\to e^-\Pi_t^+\Pi_t^-$, the total cross section at the e^+e^- linear collider can be obtained by folding $\sigma(\hat{s})$ with the photon distribution function that is given in [43, 44]:

$$\sigma(\mathrm{tot})=\int_{(2M_\Pi)^2/s}^{x_{\max}}\mathrm{d}x\sigma(\hat{s})f_\gamma(x)\,, \tag{11}$$

where

$$f_\gamma(x)=\frac{1}{D(\xi)}\left[1-x+\frac{1}{1-x}-\frac{4x}{\xi(1-x)}+\frac{4x^2}{\xi^2(1-x)^2}\right], \tag{12}$$

with

$$D(\xi)=\left(1-\frac{4}{\xi}-\frac{8}{\xi^2}\right)\ln(1+\xi)+\frac{1}{2}+\frac{8}{\xi}-\frac{1}{2(1+\xi)^2}\,. \tag{13}$$

In the above equation, $\xi=4E_e\omega_0/m_e^2$, in which m_e and E_e stand, respectively, for the incident electron mass and energy, ω_0 stands for the laser photon energy, and $x=\omega/E_e$ stands for the fraction of energy of the incident electron carried by the backscattered photon. f_γ vanishes for $x>x_{\max}=\omega_{\max}/E_e=\xi/(1+\xi)$. In order to avoid the creation of e^+e^- pairs by the interaction of the incident and backscattered photons, we require $\omega_0 x_{\max}\le m_e^2/E_e$, which implies that $\xi\le 2+2\sqrt{2}\simeq 4.8$. For the choice of $\xi=4.8$, we obtain

$$x_{\max}\approx 0.83,\quad D(\xi_{\max})\approx 1.8\,. \tag{14}$$

For simplicity, we have ignored the possible polarization for the electron and photon beams.

With the above production amplitudes, we can obtain the production cross section directly. In the calculation of the cross section, instead of calculating the square of the amplitudes analytically, we calculate the amplitudes numerically by using the method of [45, 46], which can greatly simplify our calculation.

In our calculations, we take $M_Z=91.187\,\mathrm{GeV}$, $\Gamma_Z=2.495\,\mathrm{GeV}$ and $s_\mathrm{W}^2=0.2315$ [47, 48]. The electromagnetic fine structure constant α_e at a certain energy scale is calculated from the simple QED one-loop evolution formula with the boundary value $\alpha_e=1/137.04$ [49]. Although the theory predicts top-pions to lie in the mass range of 200 GeV, this can only be regarded as a rough guide. In order to give a general prediction, we expand the mass range to 150–400 GeV.

To show the influence of the center-of-mass energy ($\sqrt{s}$) on the cross section, we take $\sqrt{s}=1.0$, 1.5 and 2.0 TeV, respectively. The numerical results of the cross section are shown in Fig. 2. One can see from Fig. 2 that the production cross section σ falls sharply as the M_Π increases. This is because the phase space is depressed strongly by a large M_Π. On the other hand, it can be concluded that the high c.m. energy is needed in order to enhance the production rate and produce enough signals. In general, the production rate is at the level of a few fb. For $\sqrt{s}=1.0\,\mathrm{TeV}$ and $150\,\mathrm{GeV}\le M_\Pi\le 300\,\mathrm{GeV}$, the value of σ is in the range of $0.23\,\mathrm{fb}\sim 10.53\,\mathrm{fb}$. If we assume that the future ILC experiment with $\sqrt{s}=1.0\,\mathrm{TeV}$ has a yearly integrated luminosity of $500\,\mathrm{fb}^{-1}$, then there will be 10^2–10^3 signals to be generated per year.

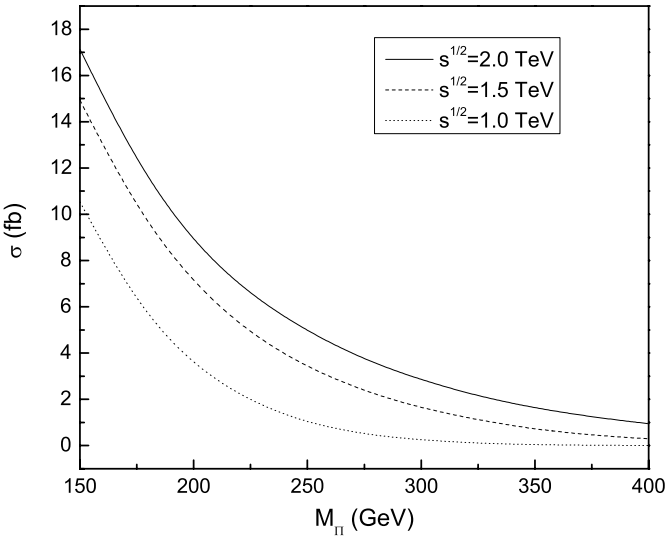

Fig. 2. The cross section of $e^-\gamma\to e^-\Pi_t^+\Pi_t^-$ versus top-pion mass M_Π for $\sqrt{s}=1.0$, 1.5 and 2.0 TeV, respectively

The most promising decay modes to search for the charged top-pions are $\Pi_t^+\to t\bar{b}$ and the flavor-charging mode $\Pi_t^+\to c\bar{b}$. In the case of $\Pi_t^+\to t\bar{b}$, the signal of the charged top-pion pair production is $t\bar{t}b\bar{b}$ plus a lepton. In order to efficiently distinguish the signals from the underlying background and to measure the top-pion mass, it is important to obtain a clean charged top-pion signal in the mass distribution of the multi-jet final states. In particular, since final states contain at least four b jets, in order to eliminate any residual QCD background, we need one or two b-tags without incurring significant penalty. Such b-tagging should have an efficiency of 60% or better. However, because of the large SM backgrounds and small production cross section for the signal process $e^-\gamma\to e^-\Pi_t^+\Pi_t^-\to e^-t\bar{t}b\bar{b}$, the possible signals of the charged top-pions are difficult to be detected via the decay channel $\Pi_t^+\to t\bar{b}$. For the light charged top-pions, the branching of $\Pi_t^+\to c\bar{b}$ is also an important mode, which induces the signals $c\bar{b}c\bar{b}$ plus a lepton. The decay branching ratio of $c\bar{b}$ is over 10% [27, 28]. Although $\Pi_t^+\to c\bar{b}$ is a FC decay mode, $c\bar{b}c\bar{b}$ production is not the flavor-changing process. Therefore, the SM background cannot be ignored. The major irreducible background should come from $e^-\gamma\to e^-ZZ$. The mistagging of b-quark and s-quark will make the process $e^-\gamma\to e^-W^+W^-$ become import-

ant, which significantly enhances the background. For $\sqrt{s} = 1 \sim 2$ TeV, the production cross section of the processes of $e^-\gamma \to e^-W^+W^-$ and $e^-\gamma \to e^-ZZ$ can reach about 10 pb and 10 fb, respectively [50, 51]. So, efficient b-tagging and c-tagging are also needed to reduce the background, the experiments can take b-tagging and c-tagging with high efficiency [52]. But a more detailed study of the background is warranted, in order to establish the experimental sensitivity to the FC coupling $\Pi_t^+ \to c\bar{b}$.

To compare the cross section of $e^-\gamma \to e^-\Pi_t^+\Pi_t^-$ with that of similar process $e^-\gamma \to e^-H^+H^-$ in the MSSM, we find that the former is significantly larger than the latter, which provides some useful information to distinguish the charged top-pions from the charged Higgs. The $t\bar{b}$ is the main decay mode for both charged top-pions and charged Higgs, and such mode is not suitable to distinguish these particles. To obtain the identified signals of the charged top-pions, we should probe charged top-pions via the flavor-changing decay mode $\Pi_t^+ \to c\bar{b}$. $\tau\nu_\tau$ can also provide the identified signals of the charged Higgs, which do not exist for the charged top-pions.

4 The processes $e^-\gamma \to \nu_e\Pi_t^-\Pi_t^0(h_t^0)$

With the couplings $\Pi_t^-\Pi_t^0W_\mu^+$ and $\Pi_t^-h_t^0W_\mu^+$, the processes $e^-\gamma \to \nu_e\Pi_t^-\Pi_t^0(h_t^0)$ can be induced at tree level. The Feynman diagrams of these process are shown in Fig. 3. The invariant production amplitudes of the process $e^-(p_1)\gamma(p_2) \to \nu_e(p_3)\Pi_t^0(p_4)\Pi_t^-(p_5)$ can be written as

$$M = M_a + M_b + M_c\,, \tag{15}$$

with

$$\begin{aligned} M_a = {} & \mathrm{i}\frac{e^3}{4\sqrt{2}s_{\mathrm{W}}^2}G(p_1-p_3,M_W)G(p_5-p_2,M_\Pi)\bar{u}(p_3)\gamma_\mu \\ & \times(1-\gamma_5)u(p_1)g^{\mu\nu}(p_5-p_2-p_4)_\nu \\ & \times(2p_3-p_2)^\rho\epsilon_\rho(p_2)\,, \end{aligned} \tag{16}$$

$$\begin{aligned} M_b = {} & \mathrm{i}\frac{e^3}{4\sqrt{2}s_{\mathrm{W}}^2}G(p_1-p_3,M_W)G(p_4+p_5,M_W)\bar{u}(p_3)\gamma_\mu \\ & \times(1-\gamma_5)u(p_1)g^{\mu\nu}\Gamma^{\nu\rho\lambda}[(p_1-p_3),\epsilon(p_2),-(p_4+p_5)] \\ & \times(p_5-p_4)_\lambda\epsilon_\rho(p_2)\,, \end{aligned} \tag{17}$$

$$\begin{aligned} M_c = {} & -\mathrm{i}\frac{e^3}{4\sqrt{2}s_{\mathrm{W}}^2}G(p_1+p_2,0)G(p_4+p_5,M_W)\bar{u}(p_3) \\ & \times(\not{p}_5-\not{p}_4)(1-\gamma_5)(\not{p}_5-\not{p}_4)\not{\epsilon}(p_2)(p_2)u(p_1)\,, \end{aligned} \tag{18}$$

where $G(p,M) = \frac{1}{p^2-M^2}$ denotes the propagator of the particles and $\epsilon_\rho(p_2)$ is the polarization vector of the photon. p_4 and p_5 denote the momenta of the outgoing neutral top-pion Π_t^0 and charged top-pion Π_t^-, repectively. In order to write a compact expression for the amplitudes, it is necessary to define the triple-boson couplings coefficient by

$$\begin{aligned} \Gamma^{\alpha\beta\gamma}(p_1,p_2,p_3) = {} & g^{\alpha\beta}(p_1-p_2)^\gamma + g^{\beta\gamma}(p_2-p_3)^\alpha \\ & + g^{\gamma\alpha}(p_3-p_1)^\beta\,, \end{aligned} \tag{19}$$

with all momenta in-coming. With the above production amplitude, we may obtain the production cross section of the process $e^-\gamma \to \nu_e\Pi_t^-\Pi_t^0$. In our numerical calculation, we will take $f_\pi = 60$ GeV, and the mass of the top-Higgs $M_H = 350$ GeV ($\approx 2m_t$). Similarly, we can also obtain the production cross section of the process $e^-\gamma \to \nu_e\Pi_t^-h_t^0$. The numerical results of the cross section are shown in Figs. 4 and 5.

It is shown that the behavior of the cross section plots of $e^-\gamma \to \nu_e\Pi_t^-\Pi_t^0(h_t^0)$ versus M_Π is similar to that of $e^-\gamma \to \nu_e\Pi_t^-\Pi_t^+$. The cross section for the process $e^-\gamma \to \nu_e\Pi_t^-\Pi_t^0$ is larger than that for the process $e^-\gamma \to \nu_e\Pi_t^-h_t^0$. In most cases, the cross section is also at the level of a few fb. For $\sqrt{s} = 1.5$ TeV and 150 GeV $\le M_\Pi \le 400$ GeV, the value of the production cross sections in the two processes are in the ranges of 0.36 fb $\sim$ 13.01 fb and 0.52 fb $\sim$ 4.68 fb, respectively. With a yearly expected luminosity about 500 fb^{-1}, there are $10^2 \sim 10^3$ signals to be generated each year.

As has been discussed, the possible decay modes of Π_t^0 are the tree-level decay modes: $t\bar{t}$ (if $\Pi_t^0 > 2m_t$), $t\bar{c}$ and

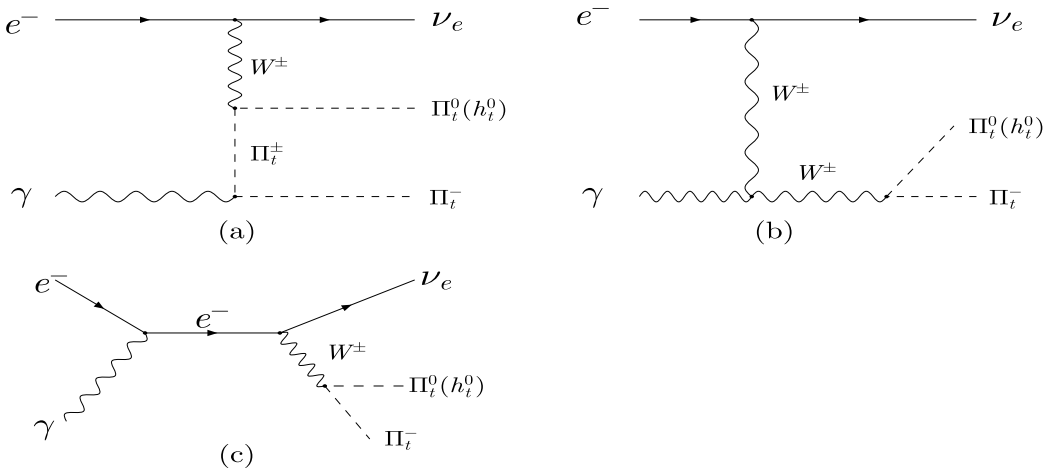

Fig. 3. The Feynman diagrams of the process $e^-\gamma \to \nu_e\Pi_t^-\Pi_t^0(h_t^0)$

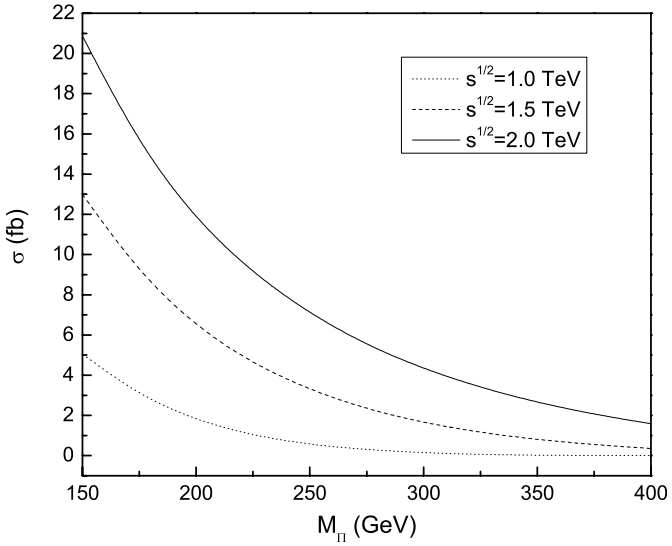

Fig. 4. The cross section of $e^-\gamma \to e^- \Pi_t^+ \Pi_t^0$ versus top-pion mass M_Π for $\sqrt{s} = 1.0, 1.5$ and 2.0 TeV, respectively

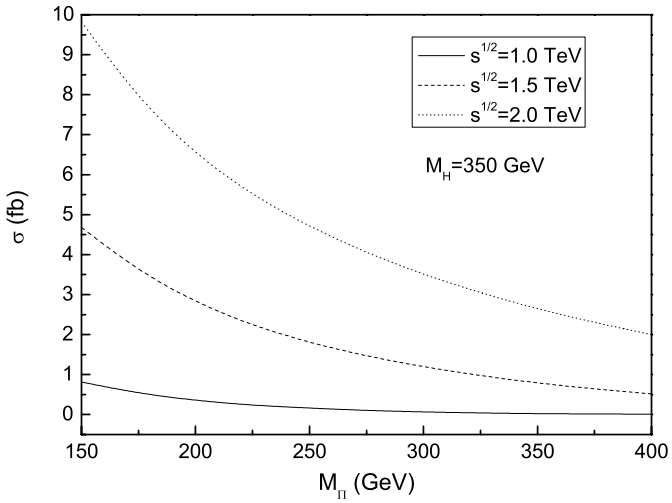

Fig. 5. The cross section of $e^-\gamma \to e^- \Pi_t^+ h_t^0$ versus top-pion mass M_Π for $M_H = 350$ GeV and $\sqrt{s} = 1.0, 1.5$ and 2.0 TeV, respectively

$b\bar{b}$, and the loop-level decay modes: gg, $\gamma\gamma$ and $Z\gamma$. As is known, the couplings of the top-pion to the three families fermions are non-universal and therefore do not posses a Glashow–Iliopoulos–Maiani (GIM) mechanism. This non-universal feature results in a large flavor-changing coupling $\Pi_t^0 t\bar{c}$. So, in the case of a light Π_t^0, the main decay mode should be $\Pi_t^0 \to t\bar{c}$. Such a decay mode involves the typical feature of the TC2 model and the peak of the invariant mass distribution of $t\bar{c}$ is narrow. With $M_H \simeq 2m_t$, the main decay modes of the top-Higgs should be tree-level modes $t\bar{c}, ZZ$ and W^+W^-. The decay rates of W^+W^-, ZZ are suppressed by $r^2 (r = m_t/v_t)$, but the branching ratio of $W^+W^- + ZZ$ can still above 10% if the decay mode $t\bar{t}$ is forbidden. These gauge boson decay modes might provide a way to distinguish h_t^0 from Π_t^0. In the SM, the cross section of the process with $t\bar{c}$ production is strongly depressed by GIM mechanism. Therefore, $\Pi_t^0(h_t^0) \to t\bar{c}$ might provide the typical signals of the TC2 model. In the MSSM, there exists a similar process, $e^-\gamma \to \nu_e H^- A^0$, which has been studied in [32, 50, 51]. The cross section is smaller than 1 fb in most of the parameter space, which provides us with some useful information to distinguish the charged top-pions from the charged Higgs. Furthermore, [50, 51] has shown that the charged Higgs bosons may be detected via the process $e^-\gamma \to \nu_e H^- A^0$ in future experiments by taking into account b-tagging capabilities. Thus, we expected that the possible signals of charged top-pions might be detected in the future LC experiments.

5 Conclusions

The SM predicts the existence of a neutral Higgs boson, while many popular models beyond the SM predict the existence of the neutral or charged scalar particles. These new particles might produce the observable signatures in current or future high-energy experiments, which is different form that for the SM Higgs boson. Any visible signal from the new scalar particles will be evidence of new physics beyond the SM. Thus, studying the new scalar particle production at the future high-energy colliders is very interesting.

The topcolor scenario is one of the important candidates for the mechanism of EWSB, A key feature of this kind of models is that they predict the existence of the top-pions $\Pi_t^{0,\pm}$ and top-Higgs h_t^0 in the low-energy spectrum. In this paper, we have computed a number of cross sections at TeV energy $e\gamma$ colliders for the production of charged top-pions in TC2 model. We find that the production rates can reach the level 10^0–10^1 fb with reasonable parameter values. The flavor-changing (FC) decay modes $\Pi_t^- \to b\bar{c}$, $\Pi_t^0(h_t^0) \to t\bar{c}$ can provide us with the typical signal to detect the top-pions and top-Higgs. Furthermore, our numerical results show that the production rates are larger than those for the charged Higgs bosons $H^\pm$ from the MSSM. Therefore, $\Pi_t^- \Pi_t^+$ and $\Pi_t^- \Pi_t^0(h_t^0)$ pair productions via the $e^-\gamma$ collision are very promising production mechanisms of the top-pions and top-Higgs in the future ILC experiments.

Acknowledgements. This work is supported in part by the National Natural Science Foundation of China (Grant No.10775039 and 10575029) and a grant from Henan Institute of Science and Technology (06040).

References

1. S. Weinberg, Phys. Rev. D **13**, 974 (1976)
2. S. Weinberg, Phys. Rev. D **19**, 1277 (1979)
3. L. Susskind, Phys. Rev. D **20**, 2619 (1979)
4. S. Dimopoulos, L. Susskind, Nucl. Phys. B **155**, 237 (1979)
5. E. Eichten, K. Lane, Phys. Lett. B **90**, 125 (1980)
6. M. Peskin, T. Takeuchi, Phys. Rev. Lett. **65**, 964 (1990)

7. J. Erler, P. Langacker, Eur. Phys. J. C **3**, 90 (1998)
8. K. Hagiwara, D. Haidt, S. Matsumoto, Eur. Phys. J. C **2**, 95 (1995)
9. C.T. Hill, Phys. Lett. B **345**, 483 (1995)
10. K. Lane, E. Eichten, Phys. Lett. B **352**, 382 (1995)
11. K. Lane, Phys. Rev. D **54**, 2204 (1996)
12. R.S. Chivukula, B.A. Dobrescu, H. Georgi, C.T. Hill, Phys. Rev. D **59**, 075 003 (1999)
13. G. Buchalla, G. Burdman, C.T. Hill, D. Kominis, Phys. Rev. D **53**, 5185 (1996)
14. G. Cvetic, Rev. Mod. Phys. **71**, 513 (1999)
15. C.-X. Yue, Q.-J. Xu, G.-L. Liu, J.-T. Li, Phys. Rev. D **63**, 115 002 (2001)
16. X.-L. Wang, W.-N. Xu, L.-L. Du, Commun. Theor. Phys. **41**, 737 (2004)
17. X.-L. Wang, Y.-L. Yang, B.-Z. Li, Phys. Rev. D **69**, 055 002 (2004)
18. X.-L. Wang et al., Phys. Rev. D **66**, 075 009 (2002)
19. X.-L. Wang, B.-Z. Li, Y.-L. Yang, Phys. Rev. D **67**, 035 005 (2003)
20. X.-L. Wang, B.-Z. Li, Y.-L. Yang, Phys. Rev. D **68**, 115 003 (2003)
21. X.-L. Wang, X.-X. Wang, Phys. Rev. D **72**, 095 012 (2005)
22. X.-L. Wang, Q.-P. Qiao, Q.-L. Zhang, Phys. Rev. D **71**, 095 012 (2005)
23. C.-X. Yue et al., Phys. Rev. D **65**, 095 010 (2002)
24. C.-X. Yue, L.-J. Liu, D.-Q. Yu, Phys. Rev. D **68**, 115 004 (2003)
25. C.-X. Yue, H. Li, X.-L. Wang, Mod. Phys. Lett. A **17**, 2349 (2002)
26. X.-L. Wang, Y.-L. Yang, B.-Z. Li, L.-D. Wan, Phys. Rev. D **66**, 075 013 (2002)
27. X.-L. Wang, L.-L. Du, W.-N. Xu, Commun. Theor. Phys. **43**, 133 (2005)
28. C.-X. Yue, Y. Jia, L.-J. Liu, X.-L. Wang, Commun. Theor. Phys. **40**, 349 (2003)
29. H.-J. He, C.P. Yuan, Phys. Rev. Lett. **83**, 28 (1999)
30. H.-J. He, S. Kanemura, C.P. Yuan, Phys. Rev. Lett. **89**, 101 803 (2002)
31. H.-J. He, S. Kanemura, C.P. Yuan, Phys. Rev. D **68**, 075 010 (2003)
32. S. Kanemura, S. Moretti, K. Odagiri, Eur. Phys. J. C **22**, 401 (2001)
33. A.K. Leibovich, D. Rainwater, Phys. Rev. D **65**, 055 012 (2002)
34. A.K. Das, C. Kao, Phys. Lett. B **372**, 106 (1996)
35. C.T. Hill, Phys. Lett. B **266**, 419 (1991)
36. Y. Nambu, EFI-89-08
37. V.A. Miransky, M. Tanabashi, K. Yamawaki, Phys. Lett. B **221**, 221 (1989)
38. W.J. Marciano, Phys. Rev. D **41**, 219 (1990)
39. G. Burdman, Phys. Rev. Lett. **83**, 2888 (1999)
40. W.A. Bardeen, C.T. Hill, M. Lindner, Phys. Rev. D **41**, 1647 (1990)
41. B. Balaji, Phys. Lett. B **393**, 89 (1997)
42. G. Burdman, D. Kominis, Phys. Lett. B **403**, 101 (1997)
43. G. Jikia, Nucl. Phys. B **374**, 83 (1992)
44. O.J.P. Eboli et al., Phys. Rev. D **47**, 1889 (1993)
45. K. Hagiwara, D. Zeppenfeld, Nucl. Phys. B **313**, 560 (1989)
46. V. Barger, H. Tao, D. Zeppenfeld, Phys. Rev. D **41**, 2782 (1990)
47. Particle Data Group, D.E. Groom et al., Eur. Phys. J. C **15**, 1 (2000)
48. Particle Data Group, K. Hagiwara et al., Phys. Rev. D **66**, 010 001 (2002)
49. J.F. Donoghue, E. Golowich, B.R. Holstein, Dynamics of the Standard Model (Cambridge University Press, Cambridge, 1992) p. 34
50. K. Cheung, Phys. Rev. D **48**, 1035 (1993)
51. K. Cheung, Nucl. Phys. B **403**, 572 (1993)
52. J.A. Conley, J. Hewett, M.P. Le, Phys. Rev. D **72**, 115 014 (2005)